Numerical model for static friction between rough elastic surfaces.

Torunn Stranden,
Department of Physics, NTNU

24th June 2003

Abstract

Motivated mainly by geophysical problems, we have developed a numerical model, that can be used to study static friction of self-affine rough elastic surfaces. As a starting point, we used a model for vertical contact, developed by Batrouni et al [1]. We extended the model to represent the whole process of static friction: two surfaces are squeezed together, and then pulled horizontally in opposite directions until they start sliding against each other. The model has been tested against known results, and show good agreement with the expected behaviour. For friction of rough elastic surfaces, we get a relatively good power-law fit: $F_{friction} \propto F_n^{\alpha}$. However, further simulations are needed to determine the coefficient α with reasonable precision.

Preface

This report presents the work that I have done for my diploma at NTNU, the Norwegian University of Science and Technology.

For my project last semester (autumn 2002), I studied the scaling properties of fracture surfaces. During this period, I became more and more interested in the geophysical applications of our work. Then, when my supervisor, professor Alex Hansen, mentioned the complexities of friction and its application to earthquakes, I found that this would be an interesting area for my diploma.

There has been some frustrating times along the way, with quite a few wrong turns. But I guess that is how research can be. All in all, I find that it has been an interesting and challenging period. I have experienced the ups and downs of numerics and programming, gained more insight in the scientific process and, of course, learned a lot about the friction of rough surfaces.

I would like to thank Alex Hansen for support and cooperation during the project period, and also for the opportunity to join the EGU-AGU-EUG general assembly in Nice in April, where we presented our work from autumn 2002. The conference was very interesting and it gave me a better understanding for the challenges in geophysics in general, and in earthquake mechanics in particular.

I would also like to thank my boyfriend Stian for being there for me.

Trondheim, 23.06.2003

Torunn Stranden

Contents

List of Figures

Chapter 1

Introduction

1.1 Motivation

The motivation behind this work has been mainly geophysical. We wished to contribute to a better understanding of the process behind earthquakes.

Earthquakes are frictional phenomena between tectonic faults or plate-interfaces [2, 3, 4, 5]. These faults and interfaces are examples of rough surfaces. Like other fracture surfaces, they are self-affine with a Hurst exponent close to 0.8 [6, 7, 8, 9, 10, 11]. Earthquakes develop via a stick-slip instability [4], where elastic strain is accumulated between the surfaces until the tension becomes too large, and there is a sudden slippage, an earthquake. This process, and thereby the friction of rough surfaces, is essential to earthquake mechanics and predictability [3].

However, there are little experimental data available on the friction of macroscopilcally rough surfaces, and more work is needed for this friction process to be fully understood. Here, the use of theoretical and numerical models plays an important part. By studying various simplified models, each trying to capture essential properties, one can gain important qualitative insights. By comparing each model's behaviour with experimental and theoretical results, and with other models, one can assess the feasability of each model, and get closer to understanding the original problem.

1.2 Objectives

Our objective has been to create a numerical model, based on the theory of elasticity, that could be used to study elastic friction between rough surfaces. As a starting point, we intended to use the model proposed by Batrouni et al [1] for vertical contact between rough surfaces. However,

we wished to extend the model to include horizontal forces and displacements. In addition, we wanted to introduce a mechanism for slip (breaking of the connections between the two surfaces), in order to be able to study the force necessary for the surfaces to start sliding against each other.

In order to establish our model, the following sub-tasks needed to be fulfilled:

- Study of relevant theory
- Design of the model
- Implementation in an appropriate programming language
- Test of the model on simple systems with known behaviour
- Study of the model's behaviour for friction of rough surfaces
- Suggestion of possible improvements and extensions to the model

1.3 Overview of the report

Section 2 contains background information about friction of rough surfaces, and gives a summary of previous work in this field. Section 3 presents relevant theory about the forces and displacements in an elastic medium. Our model for friction of rough surfaces is described in section 4, while the simulation results are presented and discussed in section 5. Section 6 presents suggested extensions and improvements to the model. Finally, section 7 contains a summary of the results and conclusions of this work.

Chapter 2

Background

Friction is an ancient field of study [12]. The first person to formulate the classical law of friction, stating that frictional force is proportional to applied load, was Leonardo Da Vinci [13, 14]. This law was later re-discovered by Guillaume Amonton [15], and is often called Amonton's 1st law.

Today, most theories assume that the frictional force is proportional to the real area of contact, that is, the sum of all contact points between the two surfaces [16, 13]. Quite a few models have been developed to study the relationship between this real contact area and the applied load. The basic mechanism is as follows: when more load is applied, the surfaces are pushed closer together. Then, new microscopic contact areas form, while the existing ones grow.

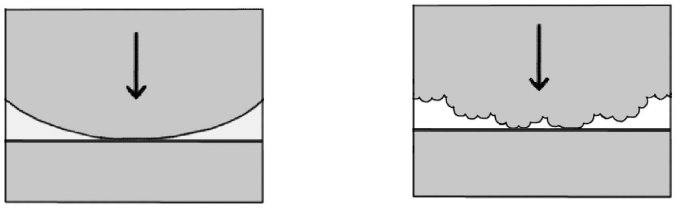

(a) Hertz contact. (b) Archard's model.

Figure 2.1: Two early models for vertical contact of rough surfaces.

In 1882, Hertz [17] found that when an elastic, spherical asperity is squeezed into a hard flat surface by a load F_n (figure 2.1 a) , the real contact area is proportional to $F_n^{2/3}$. This result has later been verified experimentally, in the case of a diamond stylus sliding on a diamond surface[18].

Archard [19] applied Hertz' solution to a fractal-like model, where small spherical asperities

was distributed on top of larger spherical asperities and so on (figure 2.1 b). Archard found that the model gave successively closer approximations to the law $A \propto F_n$ as more stages of 'asperities on top of each other' were considered. He claimed that the relationship between load and real area would be dependent on the surface topology: If the number of asperity contacts remains constant while the load is increased, the real contact area is proportional to $F_n^{2/3}$. However, if the number of asperity contacts increase with the load such that the average size of the asperity contacts remain constant, the real area of contact is proportional to F_n.

In the 1960s and 1970s, several models were studied, with results confirming Archard's theory: the relationship between load and contact area is dependent on surface topography, with $A \propto F_n^{2/3}$ and $A \propto F_n$ for the special cases mentioned above.

Greenwood and Williamson [20] developed a model where the surface was filled with hemispherical asperities, whose height varied according to a given distribution. They found that for elastic deformation and a Gaussian height distribution (which is followed rather close by many engineering surfaces) the real area of contact was almost exactly proportional to the load, thus fulfilling Amantons' 1st law. Later, several models [21, 22, 23] similar to the Greenwood and Williamson model have been studied, using various height distributions. Sometimes also the radius of the asperity tips or the density of the asperities has been varied according to some statistic distribution. The general result is that the relationship between load and real contact area follows some power law. For most 'realistic' height distributions, the exponent is found to be close to 1.

In most of the models mentioned, each surface asperity is supposed to be independent: the forces on one asperity does not change the geometry of another. Also, roughness is introduced only on a single length-scale or on a small range of length-scales. These are reasonably good approximations for polished surfaces and other surfaces where the relevant length scale is much higher than the large-scale self-affine cutoff length of the material. Several experiments [24, 25] support, with reasonable precision, the relationship $A \propto F_n$ for such surfaces. For self-affine surfaces with high large-scale cutoff lengths, however, the approximations does not hold true. In such systems, roughness on virtually all length-scales are important, and the asperities deform dependently of each other.

In 2001, Persson [26, 27] published a theory where he studied vertical contact for randomly rough surfaces. He found that in the framework of his model, the real contact area is in most cases proportional to F_n. However, in a numerical work published in 2002, Batrouni et al [1] found that $F_n \propto A^{1.1} \Rightarrow A \propto F_n^{0.91}$ for self-affine rough surfaces, using a model based on the equations of elasticity.

In a frictional process, both vertical and horizontal forces and displacements are involved.

However, most of the models used to study real area of contact look at vertical contact only, and most of the models ignore shear-forces. Also, when used to explain friction, most models take for granted that the frictional force is proportional to the real contact ares. In this work, we have extended the model of Batrouni et al [1] to include horizontal forces and displacements, and to represent the whole process of static friction: two surfaces are squeezed together, and then pulled horizontally in opposite directions until they start sliding against each other.

Chapter 3

Theory of elasticity: Forces and displacements.

The theoretical background for our model is the theory of elasticity. This theory describes how continuous media deform elastically due to applied forces. Elastic deformations are reversible: an elastic medium returns to its original size and shape when all applied stresses are removed. See for example Landau and Lifshitz [28] for more about the theory of elasticity.

When the deformation of a body is caused by forces applied to its surface, theory of elasticity provides the following equation of equilibrium [28]:

$$(1-2s)\bigtriangleup \mathbf{u} + \bigtriangledown(\bigtriangledown \cdot \mathbf{u}) = 0 \tag{3.1}$$

where $\mathbf{u}$ is the deformation in a point, and s is Poison's ratio. The equation of equilibrium (3.1) holds throughout the space occupied by the elastic medium.

3.1 Elastic half-space subject to a point force

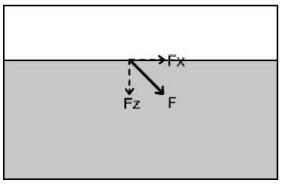

Figure 3.1: Elastic half-space subject to a point force.

Let us consider an elastic half-space subject to a point force in the x-z plane, as illustrated in figure 3.1. The equation of equilibrium can then be solved to find the deformation as a function of position. We take origin to be the point where the point force hits the media. At the surface (z=0), we then get the following solution [28]:

$$\begin{aligned} u_z(x,y) &= \frac{1+s}{2\pi E}\left\{\frac{2(1-s)}{r}F_z + \frac{(1-2s)x}{r^2}F_x\right\} \\ u_x(x,y) &= \frac{1+s}{2\pi E}\left\{-\frac{(1-2s)x}{r^2}F_z + \left(\frac{2(1-s)}{r} + \frac{2s}{r^3}\right)F_x\right\} \end{aligned} \tag{3.2}$$

where $r = \sqrt{x^2+y^2}$and E is Young's modulus.

3.2 Elastic half-space subject to a general stress-field

The elastic equations (3.2) for a point force on an elastic half-plane can be integrated up to be valid for any stress-field σ on the elastic half-plane surface:

$$\begin{aligned} u_z(x,y) &= \int\int (G_{zz}(x-x',y-y')\sigma_z(x',y') + G_{zx}(x-x',y-y')\sigma_x(x',y'))dx'dy' \\ u_x(x,y) &= \int\int \left(G_{xz}(x-x',y-y')\sigma_z(x',y') + G_{xx}(x-x',y-y')\sigma_x(x',y')\right)dx'dy' \end{aligned} \tag{3.3}$$

where the Green functions are found from equation (3.2):

$$\begin{aligned} G_{zz}(l,m) &= \frac{(1-s^2)}{\pi E}\cdot\frac{1}{\sqrt{l^2+m^2}} \\ G_{zx}(l,m) &= \frac{(1+s)(1-2s)}{2\pi E}\cdot\frac{u}{(l^2+m^2)} \\ G_{xz}(l,m) &= -\frac{(1+s)(1-2s)}{2\pi E}\cdot\frac{u}{(l^2+m^2)} \\ G_{xx}(l,m) &= \frac{(1-s^2)}{\pi E}\cdot\frac{1}{\sqrt{l^2+m^2}} + \frac{s(1-s)}{\pi E}\cdot\frac{1}{(l^2+m^2)^{3/2}} \end{aligned}$$

with $l = x - x'$ and $m = y - y'$.

3.3 Discretization of the elastic equations

To use the elastic equations (3.3) in our numerical model, they need to be discretizised. This can be done by averaging over an area a^2 which corresponds to the discretization size of the grid that represent the elastic half-plane.

The resulting discrete equations are as follows:

$$\begin{aligned} u_{z,(i,j)} &= \sum_{i'}\sum_{j'} \overline{G}_{zz,(i-i',j-,j')} f_{z,(i',j')} + \overline{G}_{zx,(i-i',j-,j')} f_{x,(i',j')} \\ u_{x,(i,j)} &= \sum_{i'}\sum_{j'} \overline{G}_{xz,(i-i',j-,j')} f_{z,(i',j')} + \overline{G}_{xx,(i-i',,j-j')} f_{x,(i',j')} \end{aligned} \tag{3.4}$$

The computation of the discrete Green functions $\overline{G}_{zz}, \overline{G}_{zx}, \overline{G}_{xz}$ and $\overline{G}_{xx}$ is found in Appendix A. If we set $l = x - x' = a \cdot (i - i')$ and $m = y - y' = a \cdot (j - j')$ where a is the lattice spacing, we get the following expressions:

$$\begin{aligned} \overline{G}_{zz}(l,m) &= \frac{1}{a^2} \cdot \frac{1-s^2}{\pi E} \cdot \Bigg\{ (l+a/2) \cdot ln \left(\frac{m+a/2+\sqrt{(m+a/2)^2+(l+a/2)^2}}{m-a/2+\sqrt{(m-a/2)^2+(l+a/2)^2}} \right) \\ &\quad +(m+a/2) \cdot ln \left(\frac{l+a/2+\sqrt{(m+a/2)^2+(l+a/2)^2}}{l-a/2+\sqrt{(m+a/2)^2+(l-a/2)^2}} \right) \\ &\quad +(l-a/2) \cdot ln \left(\frac{m-a/2+\sqrt{(m-a/2)^2+(l-a/2)^2}}{m+a/2+\sqrt{(m+a/2)^2+(l-a/2)^2}} \right) \\ &\quad + (m-a/2) \cdot ln \left(\frac{l-a/2+\sqrt{(m-a/2)^2+(l-a/2)^2}}{l+a/2+\sqrt{(m-a/2)^2+(l+a/2)^2}} \right) \Bigg\} \end{aligned}$$

$$\begin{aligned} \overline{G}_{zx}(l,m) &= \frac{1}{a^2} \cdot \frac{(1+s)(1-2s)}{2\pi E} \cdot \Bigg\{ \frac{1}{2}(m+a/2) \cdot ln \left(\frac{(l+a/2)^2+(m+a/2)^2}{(l-a/2)^2+(m+a/2)^2} \right) \\ &\quad +\frac{1}{2}(m-a/2) \cdot ln \left(\frac{(l-a/2)^2+(m-a/2)^2}{(l+a/2)^2+(m-a/2)^2} \right) \\ &\quad +(l+a/2) \cdot \left(arctan \left(\frac{m+a/2}{l+a/2} \right) - arctan \left(\frac{m-a/2}{l+a/2} \right) \right) \\ &\quad +(l-a/2) \cdot \left(arctan \left(\frac{m-a/2}{l-a/2} \right) - arctan \left(\frac{m+a/2}{l-a/2} \right) \right) \Bigg\} \end{aligned}$$

$$
\begin{aligned}
\overline{G}_{xz}(l,m) &= -\frac{1}{a^2}\cdot\frac{(1+s)(1-2s)}{2\pi E}\cdot\left\{\frac{1}{2}(m+a/2)\cdot ln\left(\frac{(l+a/2)^2+(m+a/2)^2}{(l-a/2)^2+(m+a/2)^2}\right)\right. \\
&+\frac{1}{2}(m-a/2)\cdot ln\left(\frac{(l-a/2)^2+(m-a/2)^2}{(l+a/2)^2+(m-a/2)^2}\right) \\
&+(l+a/2)\cdot\left(arctan\left(\frac{m+a/2}{l+a/2}\right)-arctan\left(\frac{m-a/2}{l+a/2}\right)\right) \\
&\left.+(l-a/2)\cdot\left(arctan\left(\frac{m-a/2}{l-a/2}\right)-arctan\left(\frac{m+a/2}{l-a/2}\right)\right)\right\}
\end{aligned}
$$

$$
\begin{aligned}
\overline{G}_{xx}(u,v) &= \frac{1}{a^2}\cdot\frac{1+s}{\pi E}\cdot\left\{(m+a/2)\cdot ln\left(\frac{l+a/2+\sqrt{(m+a/2)^2+(l+a/2)^2}}{l-a/2+\sqrt{(m+a/2)^2+(l-a/2)^2}}\right)\right. \\
&+(m-a/2)\cdot ln\left(\frac{l-a/2+\sqrt{(m-a/2)^2+(l-a/2)^2}}{l+a/2+\sqrt{(m-a/2)^2+(l+a/2)^2}}\right) \\
&+(1-s)(l+a/2)\cdot ln\left(\frac{m+a/2+\sqrt{(m+a/2)^2+(l+a/2)^2}}{m-a/2+\sqrt{(m-a/2)^2+(l+a/2)^2}}\right) \\
&\left.+(1-s)(l-a/2)\cdot ln\left(\frac{m-a/2+\sqrt{(m-a/2)^2+(l-a/2)^2}}{m+a/2+\sqrt{(m+a/2)^2+(l-a/2)^2}}\right)\right\}
\end{aligned}
$$

3.4 Vector formulation

When we have discrete data, we can choose between using vectors or matrixes to represent positions, forces and displacements. For example, if we have a $N \times N$ matrix to start with, the same information can be contained in a vector of length N^2. Using vector formulation, equation (3.4) can be re-formulated:

$$
\begin{aligned}
\mathbf{u}_z &= \overline{\mathbf{G}}_{zz}\cdot\mathbf{f}_x + \overline{\mathbf{G}}_{zx}\cdot\mathbf{f}_x \\
\mathbf{u}_x &= \overline{\mathbf{G}}_{xz}\cdot\mathbf{f}_z + \overline{\mathbf{G}}_{xx}\cdot\mathbf{f}_x
\end{aligned}
\tag{3.5}
$$

Here, $\overline{\mathbf{G}}_{zz}$, $\overline{\mathbf{G}}_{zx}$, $\overline{\mathbf{G}}_{xz}$ and $\overline{\mathbf{G}}_{xx}$ are 2D matrixes which contain the Green functions as function of two positions: r and r'. The variable r includes information of both x and y (if x goes from 1 to N, r goes from 1 to N^2).

Chapter 4

Model for static friction of rough surfaces

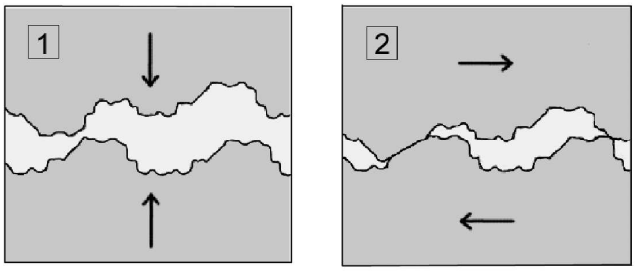

(a) First, the surfaces are squeezed together vertically.

(b) Then, they are pulled horizontally in opposite directions.

Figure 4.1: Original system: two rough elastic surfaces are squeezed together, and then pulled in separate directions horizontally.

The original system that we want to study consists of two large blocks of elastic media, each with a rough surface. The two blocks are first squeezed together vertically, and then pulled in separate directions horizontally, until they 'slip' and start gliding along each other. This is illustrated in figure 4.1.

4.1 Simplified system

It has been shown [29, 30] that many of the characteristics of the system in figure 4.1 is captured by a simpler setting where an equivalent elastic, rough surface is pushed into a hard plane surface.

This is a useful system to work with, and the results is directly comparable to earlier work, since most earlier models also has used such a system.

We wish to take the modification somewhat further, and use a system where a hard, rough surface is pushed into an elastic plane surface. This makes the equations of elasticity for an elastic half-plane more obviously applicable. This simplified system is shown in figure 4.2.

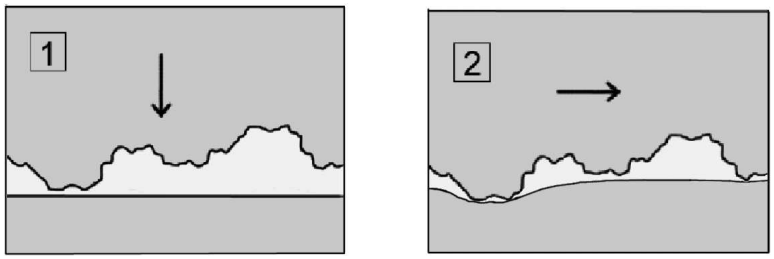

(a) First, the rough surface is squeezed into the elastic halfplane

(b) Then, it is pulled horisontally

Figure 4.2: Simplified system: a hard, rough surface is squeezed into an elastic half-plane, and then pulled horizontally.

The change from two elastic rough surfaces to one hard rough surface that is pushed into an elastic half-plane will modify the behaviour of the system somewhat [29]. But we believe that it is an useful system to work with, and that the results will give us improved qualitative understanding, also of the original system.

4.2 Discrete representation of the surfaces

We represent both surfaces as two-dimensional $L \times L$ lattices, with a discretization size a that corresponds to the low-scale self-affine cutoff length of the rough surface. The rough surface is described by its vertical profile $\{z_{i,j}\}$, while the elastic half-plane is described by the displacements at each point: $\{u_{i,j}\}$.

The two-dimensional lattices could easily be implemented as 2d matrixes with dimension $N \times N$ (where $N = \frac{L}{a}$). However, we choose an alternative approach where equation 3.5 can be used directly. For each surface, we introduce a vector of length N^2 where the vector positions corresponds to positions in the original $L \times L$ lattice. The matrix- and vector- formulations are equivalent. If the indices of the matrix are i and j, and the numbering start at 1, one can go from one formulation to the other as follows : $matrix(i, j) = vector(i + N \cdot j)$.

4.3 Numerical generation of self-affine rough surfaces

In Fourier space, 2d self-affine surfaces has the power spectrum $P(k) \sim \frac{1}{k^{2+2H}}$. This can be utilised to generate self-affine surfaces (see also[31]):

- Fill the L x L grid with white noise (random numbers)
- Fourier transform the grid, using a discrete 2d fast Fourier transform
- Filter the data, by multiplying each value (both the real and the imaginary part) with $\frac{1}{\left(\sqrt{k_x^2+k_y^2}\right)^{(H+1)}}$.
- Transform the grid back to normal space, using the inverse 2d fast Fourier transform

An example of a rough surface produced by this two-dimensional Fourier method, is shown in figure 4.3.

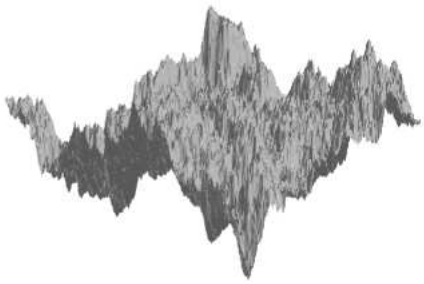

Figure 4.3: Rough surface generated using a two-dimensional Fourier method.

4.4 De-coupling of the elastic equations

In section 3.3, we found discrete elastic equations (3.5) that can be used to find the forces and displacements of our elastic half-plane.

The system can be greatly simplified if we can ignore the coupling between vertical and horizontal forces and displacements. If we assume that the coupling is weak, so that the coupling-terms can be ignored, equation (3.5) becomes two relatively simple, independent relations:

$$\mathbf{u}_z = \overline{\mathbf{G}}_{zz} \cdot \mathbf{f}_z \tag{4.1}$$

$$\mathbf{u}_x = \overline{\mathbf{G}}_{xx} \cdot \mathbf{f}_x \tag{4.2}$$

Having removed the link between horizontal and vertical effects, we can divide the friction process into two independent stages:

1. Vertical squeeze:
   The rough surface is squeezed a distance D_z into the elastic, flat medium. This correspond to the model used by Batrouni et al [1].

2. Horizontal pull:
   Having obtained the contact area from 1., we pull the rough surface a distance D_x horizontally. Using the obtained force distributions horizontally and vertically, we can also simulate a 'slip' process, where the horizontal forces overcome the vertical ones, and the rough surface starts sliding.

4.5 Vertical squeeze

Figure 4.4: A rough surface is pushed vertically into an elastic, flat medium, until it reaches a given penetration depth D_z. The dashed, horizontal line represents the undeformed elastic medium.

The first stage of our friction process is the vertical squeeze, modelled by Batrouni et al [1]. As shown in figure 4.4, we squeeze the rough surface into the elastic flat medium, until the normal distance between the point of first contact to the undeformed surface of the flat medium equals a given penetration depth D_z.

4.5.1 Boundary conditions

To be able to solve the elastic equation (4.1) for our system, the boundary conditions need to be established. We have the following known quantities:

1. Displacements: Knowing the profile of the rough surface, and given the penetration depth D_z, the displacements$\{u_z\}$ of the elastic medium is defined at all points where the two surfaces are in contact.

2. Forces: At the points where the surfaces are not in contact, the elastic surface deform in response to the influences from the contact regions. Equilibrium is reached when the net force vanish. Therefore, at points with no contact, the forces f_k equal zero.

We introduce a diagonal $L^2 \times L^2$ contact matrix $\mathbf{K_z}$with elements equal to 1 on contact-sites, and to 0 at no-contact sites. The boundary conditions 1. and 2. can then be formulated as:

$$\begin{aligned} \mathbf{K_z} \cdot \mathbf{u_z} &= \begin{cases} 0 & at\ points\ with\ no\ contact \\ u_{z,imposed} & at\ contact\ points \end{cases} \\ (\mathbf{I} - \mathbf{K_z}) \cdot \mathbf{f_z} &= 0 \quad everywhere \end{aligned} \tag{4.3}$$

where I is the identity matrix.

4.5.2 Solving the elastic equation

The elastic equation (4.1) can be rewritten as:

$$\overline{\mathbf{G}}_{\mathbf{zz}} \cdot (\mathbf{I} - \mathbf{K_z}) \cdot \mathbf{f_z} + \overline{\mathbf{G}}_{\mathbf{zz}} \cdot \mathbf{K_z} \cdot \mathbf{f_z} = (\mathbf{I} - \mathbf{K_z}) \cdot \mathbf{u_z} + \mathbf{K_z} \cdot \mathbf{u_z}$$

this form is convenient, because it facilitates inclusion of the boundary conditions directly into the equation. We see from equation (4.3) that $\mathbf{K_z} \cdot \mathbf{u_z}$ is known everywhere, and that $(\mathbf{I} - \mathbf{K_z}) \cdot \mathbf{f_z}$ is zero everywhere. Putting the unknowns on the left-hand side, we obtain:

$$\overline{\mathbf{G}}_{\mathbf{zz}} \cdot \mathbf{K_z} \cdot \mathbf{f_z} - (\mathbf{I} - \mathbf{K}_z) \cdot \mathbf{u_z} = \mathbf{K_z} \cdot \mathbf{u_z} \tag{4.4}$$

We define a vector $\mathbf{x_z} = \mathbf{K_z} \cdot \mathbf{f_z} + (\mathbf{I} - \mathbf{K_z}) \cdot \mathbf{u_z}$. The vector $\mathbf{x_z}$ then represents all the unknown quantities in our system:

$$\mathbf{x_z} = \begin{cases} u_z & at\ points\ with\ no\ contact \\ f_z & at\ contact\ points \end{cases}$$

By the definition of $\mathbf{K}_z$ and $\mathbf{I}$, we have that $(\mathbf{I}-\mathbf{K_z})\cdot\mathbf{K_z} = \mathbf{K_z}\cdot(\mathbf{I}-\mathbf{K_z}) = \mathbf{0}$, that $\mathbf{K_z}\cdot\mathbf{K_z} = \mathbf{K_z}$ and that $(\mathbf{I}-\mathbf{K_z})\cdot(\mathbf{I}-\mathbf{K_z}) = (\mathbf{I}-\mathbf{K_z})$. Using this, we get from equation (4.4):

$$\begin{aligned} \overline{\mathbf{G}}_{\mathbf{zz}}\cdot\mathbf{K_z}\cdot\mathbf{x_z} - (\mathbf{I}-\mathbf{K_z})\cdot\mathbf{x_z} &= \mathbf{K_z}\cdot\mathbf{u_z} \\ &\Downarrow \\ \left(-\mathbf{I} + \left(\mathbf{I}+\overline{\mathbf{G}}_{zz}\right)\cdot\mathbf{K_z}\right)\cdot\mathbf{x_z} &= \mathbf{K_z}\cdot\mathbf{u_z} \end{aligned} \tag{4.5}$$

Equation (4.5) is on the form Ax=b, and can be solved using, for example, the conjugate gradient method [32].

4.5.3 Real contact area

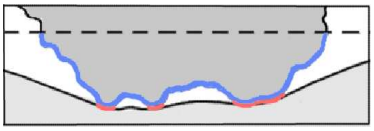

Figure 4.5: As the rough surface is pushed into the elastic, flat medium, the elastic media deform. The real contact area (red) is not equal to the 'slice area' (blue).

One problem remains. The real contact area, which defines $\mathbf{K_z}$, is not known. A first estimate for the contact area might be the 'slice area', the area obtained by taking a cut trough the rough surface. However, as seen in figure 4.5, this contact-area estimation will be inaccurate. As we push the rough surface into the elastic one, the latter deform, and the contact area becomes significantly smaller than the 'slice area'.

We find the correct contact area, by using an iteration procedure:

1. Initially, use the 'slice area' as an estimate. Forcing this contact area upon the system, solve equation (4.5), and obtain the forces and displacement of the elastic solid.

2. When the elastic equation is solved with a too large contact area, some of the forces obtained will be negative. In these points, the elastic surface tries to pull away from the rough

surface. Update the contact area by setting $K_z = 0$ at the elements corresponding to sites where $f_z < 0$.

3. Solve equation (4.5) with the new contact area. If there are still negative forces, go back to 2) and update $\mathbf{K_z}$ again. Repeat this process until there are no negative forces.

After we have solved equation (4.5) with the final $\mathbf{K_z}$, we have a solution of both the vertical force distribution and the real contact area of our system, given the rough surface profile and the penetration depth D_z.

4.6 Horizontal pull

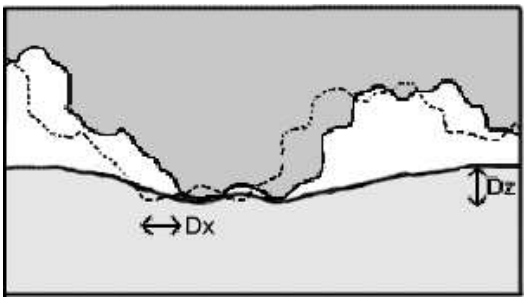

Figure 4.6: A rough surface, already squeezed a distance D_z into an elastic medium, is pulled horizontally a distance D_x. The dashed line represents the position of the rough surface before the horizontal movement.

Our rough surface has now been squeezed vertically a distance D_z into the elastic medium. It is time for the next stage of our process: the horizontal pull. Keeping the vertical forces constant (due to the de-coupling of the elastic equation, the vertical forces and deformations are independent to the horizontal ones), we pull the rough surface a distance D_x horizontally relative to the elastic medium.

4.6.1 Boundary conditions

Again, we need to establish boundary conditions, to be able to solve the elastic equation (4.2). We have the following known quantities:

1. Displacements: Everywhere where the elastic medium is bound to the rough surface, it is pulled a distance D_x horizontally. On all such 'bound' sites, the deformations u_x equals D_x.

2. Forces: At the points where the surfaces are not bound to each other, the elastic surface is free to deform horizontally in response to the influences from the fastened regions. Equilibrium is reached when the net force vanish. Therefore, at 'free' sites, the forces f_x equal zero.

We introduce a diagonal L^2xL^2 matrix $\mathbf{K_x}$with elements equal to 1 on bound sites, and to 0 at free sites. The boundary conditions 1. and 2. can then be formulated as:

$$\begin{aligned} \mathbf{K_x} \cdot \mathbf{u_x} &= \begin{cases} 0 & at\ free\ sites \\ D_x & at\ bound\ sites \end{cases} \\ (\mathbf{I} - \mathbf{K_x}) \cdot \mathbf{f_x} &= 0 \quad everywhere \end{aligned} \tag{4.6}$$

where I is the identity. Initially, the two surfaces will be bound together everywhere where they are in contact: $\mathbf{K_{x0}} = \mathbf{K_z}$.

4.6.2 Solving the elastic equation

Using the boundary conditions (4.6) , we can, via the same procedure as in section 4.5.2, reformulate the elastic equation (4.2) to the following:

$$\left(-\mathbf{I} + \left(\mathbf{I} + \overline{\mathbf{G}}_{xx}\right) \cdot \mathbf{K_x}\right) \cdot \mathbf{x_x} = \mathbf{K_x} \cdot \mathbf{u_x} \tag{4.7}$$

with $\mathbf{x_x} = \mathbf{K_x} \cdot \mathbf{f_x} + (\mathbf{I} - \mathbf{K_x}) \cdot \mathbf{u_x}$. Equation (4.7) is on the form Ax=b, and can be solved using, for example, the conjugate gradient method [32].

4.6.3 Slip - breaking the bonds between the surfaces

Once the horizontal forces overcome some threshold, the bonds between the two surfaces should break down, and the rough surface should start sliding along the elastic one. We wish to establish an algorithm for this 'slip' process.

We introduce a local friction constant λ, defined as follows: if $f_x > \lambda f_z$ at some lattice site, the 'bond' between the surfaces at this site will break. The horizontal deformation of the elastic surface will then adjust itself, so that the total horizontal force at the new 'free' site equals zero. In our simulations we have used $\lambda = constant = 0.2$.

The problem is that we do not initially know the distance D_x necessary for the first bond to break. However, we can assume that the force-distribution $\{f_x\}$ is a piecewise linear function of D_x: the relationship is linear on the intervals where both the vertical contact area and the horizontally "bound" area are constant. Furthermore, due to the de-coupling of the elastic equations, the linear functions $f_x(D_x)$ go through zero. With no horizontal displacements $(D_x = 0)$, there are no horizontal forces $(f_x = 0)$.

We simulate the slip-process, using the following iterative model:

1. Define a penetration depth D_z. Using the algorithm described in section 4.5, find the vertical force distribution $\{f_z\}$, the total vertical force $F_n = \sum f_z$ and the contact area $\mathbf{K_z}$
2. Initially, set $\mathbf{K_x}$= $\mathbf{K_z}$.
3. Introduce a small horizontal movement D_x. Find the horizontal force distribution $\{f_x\}$ and the total horizontal force $F_x = \sum f_x$, solving equation (4.7).
4. Find the site where the fraction $\frac{f_x}{\lambda f_z}$ has its maximum value. This will be the first 'bond' to break.
5. Update $\mathbf{K_x}$, setting $K_x = 0$ at the element corresponding to the broken 'bond'.
6. Find the total horizontal force $F_{x,lim}$ needed to break the chosen 'bond'. Assuming a linear relationship between $\{f_x\}$ and D_x, going through zero, $F_{x,lim}$relates to F_x as 1 relates to $max\left\{\frac{f_x}{\lambda f_z}\right\}$. This implies the following scaling relation: $F_{x,lim} = F_x \cdot \frac{1}{max\left\{\frac{f_x}{\lambda f_z}\right\}}$.
7. Repeat from 2. until all 'bonds' have broken.

When all bonds are broken, using the process 1.-5., the elastic surface is no longer bound to the rough one, and the rough surface start sliding. The static friction force is defined as the force needed to make this happen:

$$F_{friction} \quad = \quad max\left\{F_{x,lim}\right\}$$

4.7 Summary: Algorithm

1. Squeeze

   (a) Generate a rough surface

   (b) Define a penetration depth D_z

   (c) u_z is now defined everywhere where there is contact, and $f_z = 0$ everywhere where there is no contact

   (d) Set initial contact area $\mathbf{K_z}$ equal to the slice area (see figure 4.5).

   (e) Solve the elastic equation, $\left(-\mathbf{I} + \left(\mathbf{I} + \overline{\mathbf{G}}_{zz}\right) \cdot \mathbf{K_z}\right) \cdot \mathbf{x_z} = \mathbf{K_z} \cdot \mathbf{u_z}$ with respect to $\mathbf{x_z}$, to obtain the vertical forces $\{f_z\}$ and displacements $\{u_z\}$

   (f) Iterate. If there exists points where $f_z < 0$:

      i. set $K_z = 0$ at these points

      ii. return to (e)

   (g) We now know the contact area, the vertical force distribution $\{f_z\}$ and the total vertical force $F_n = sum\{f_z\}$

2. Pull and slip

   (a) Initially, set the stick area $\mathbf{K_x}$ equal to the contact area $\mathbf{K_z}$

   (b) Introduce a small horizontal pulling-distance D_x

   (c) Now, $u_x = D_x$ everywhere where there is stick, and $f_x = 0$ everywhere where there is no stick

   (d) Solve the elastic equation, $\left(-\mathbf{I} + \left(\mathbf{I} + \overline{\mathbf{G}}_{xx}\right) \cdot \mathbf{K_x}\right) \cdot \mathbf{x_x} = \mathbf{K_x} \cdot \mathbf{u_x}$ with respect to $\mathbf{x_x}$, to obtain the horizontal forces $\{f_x\}$ and displacements $\{u_x\}$

   (e) Calculate the total horizontal force $F_x = sum\{f_x\}$

   (f) Iterate. While there exists points where $K_x = 1$:

      i. Find the point with the maximum fraction $\frac{f_x}{\lambda f_z}$

      ii. set $K_x = 0$ at this point

      iii. find $F_{x,lim} = F_x \cdot \frac{1}{max\left\{\frac{f_x}{\lambda f_z}\right\}}$

      iv. return to (e).

   (g) Find the friction force $F_{friction} = max\{F_{x,lim}\}$

3. Return to 1. and repeat on a defined number of samples. Average the results over the samples, to find a point in the static friction law $F_{friction} = F_{friction}(F_n)$

4. Return to 1 with another penetration depth D_z

Chapter 5

Numerical simulations

5.1 Hertz vertical contact

First, we wanted to test our model, by using it on a simple system with known results. We decided to use the Hertz contact problem for this purpose. The Hertz system consists of a single, spherical asperity that is pushed vertically into a flat surface (see figure 2.1 a). We used the procedure described in section 4.5, to find the relationship between D_z and F_n for such a system. The results are plotted in figure 5.1.

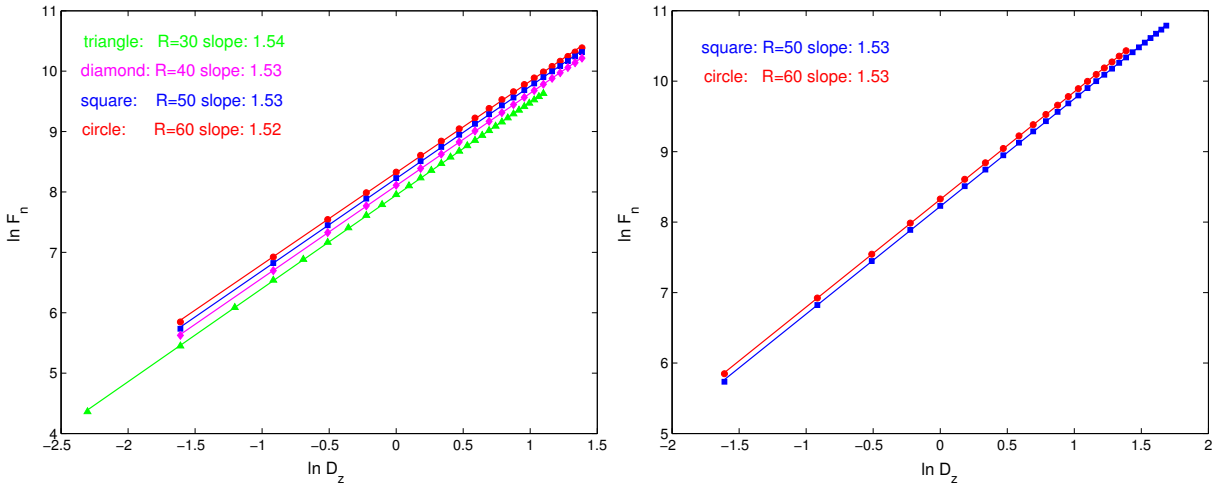

(a) N=24

(b) N=32

Figure 5.1: Results for vertical Hertz contact for two different grid sizes: (a) N=24, (b) N=32

The vertical Hertz contact problem has an exact solution [17, 18]: $D_z \propto F_n^{2/3}$. Our simulations gave $F_n \propto D_z^{1.53\pm0.1} \Rightarrow D_z \propto F_n^{0.65\pm0.1}$, in good agreement with the exact relationship. The small difference can be explained by finite size effects.

5.2 Hertz friction

We also wished to see how the Hertz system behave using our full friction model. The resulting relationship between F_n and $F_{friction}$ is plotted in figure 5.2.

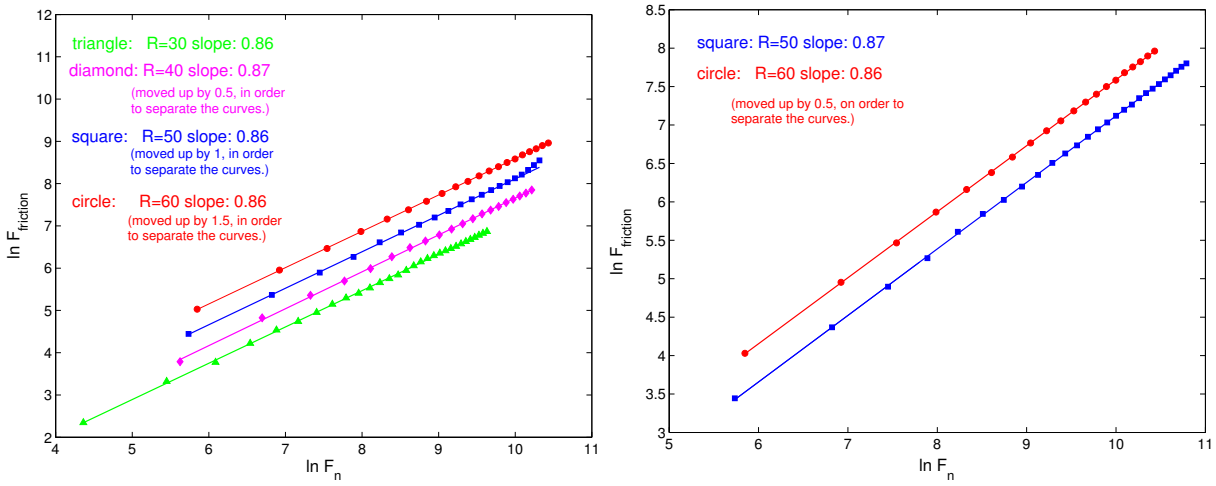

(a) N=24

(b) N=32

Figure 5.2: Results for Hertz friction. Some of the curves are moved up by a constant value, to separate the curves from eachother. (a) N=24, (b) N=32

Our simulation results fit well to a power law dependence $F_{friction} \propto F_n^{\alpha}$, with $\alpha = 0.86\pm0.1$ for these grid sizes. There might however be finite size effects, and simulation on larger systems (both larger L and larger R) is needed, to find a reliable value for α as $N \to \infty$. However, an interesting observation is that the measured α is not equal to 2/3. It seems like the inclusion of horizontal effects has moved the exponent closer to 1, compared to a purely vertical consideration where $F_{friction} \propto A$ is assumed.

5.3 Rough surfaces in vertical contact

Having tested the model on the relatively simple Hertz system, we now wished to study self-affine rough surfaces in contact. First, we looked at the vertical problem: a rough surface is pushed vertically into an elastic medium (see figure 4.4). The results are found in figure 5.3.

We chose surfaces with Hurst exponents 0.8 and 0.6 as subject for our simulation, both because $H \approx 0.8$ for fracture surfaces, and because $H = 0.8$ and $H = 0.6$ were the values used by Batrouni et al [1], thus making the results more comparable.

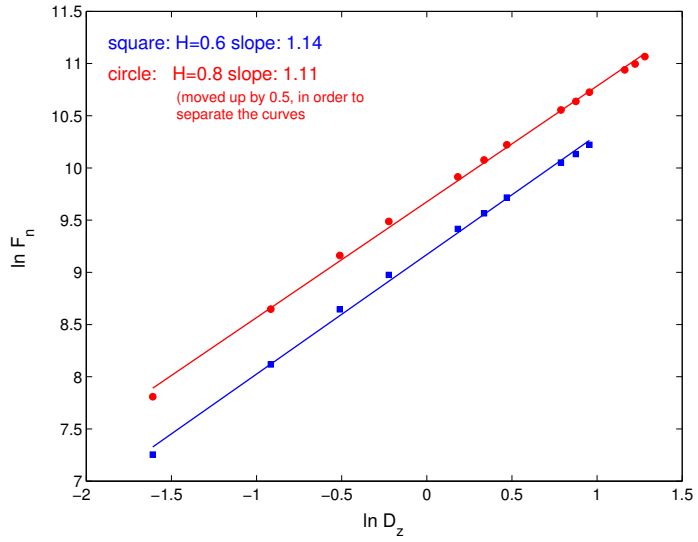

Figure 5.3: Results for rough surfaces in vertical contact. Grid size: N=24. One of the curves is moved up by a constant value, to separate the curves from each other.

Again, our data gives a relatively good power-law fit $F_n \propto D_z^{\beta}$. The measured exponents are $\beta \approx 1.14$ for $H = 0.6$ and $\beta \approx 1.11$ for $H = 0.8$ with system size $N = 24$. However, with only 5 samples at each data-point, the values for β have high uncertainties.

Batrouni et al [1], found the relationship $F_n \propto D_z^{2.25}$ for $H = 0.6$ and $F_n \propto D_z^{2.05}$ for $H = 0.8$, by extrapolating to $L \to \infty$. However, they found large finite size effects, with β significantly decreasing for decreasing system size. Batrouni et al have not published any value for β at $L = 24$. However, a β value slightly above 1.1 for $L = 24$, and $\beta(H = 0.6) > \beta(H = 0.8)$ fit quite well with the trend of their results.

5.4 Friction of rough surfaces

Finally, we used our model to simulate the static friction of rough surfaces. The results are found in figure 5.4.

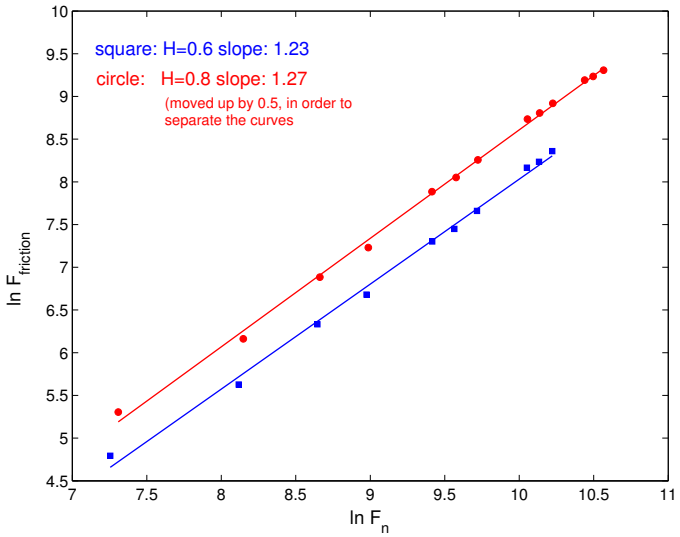

Figure 5.4: Results for friction of rough surfaces. Grid size: N=24. One of the curves is moved up by a constant value, to separate the curves from each other.

We found a relatively good power-law fit, with exponents are $\alpha \approx 1.23$ for $H = 0.6$ and $\alpha \approx 1.27$ for $H = 0.8$ with system size L=24.

These results are interesting, as they provide a non-linear relationship between load and frictional force. However, there are large uncertainties, and the finite size effects might be large. Simulations on several, larger system sizes and with many more samples is needed, to be able to say anything conclusive about the friction of rough surfaces.

Chapter 6

Suggested extensions and improvements to the model

6.1 Coupled effects

In section 4.4, we made the assumption that the coupling between vertical and horizontal forces and displacements is weak. Therefore, we could ignore the coupling-terms in the elastic equations.

It would, however, be interesting to see how the model would behave with the whole equations included. If we could compare simulation-results for the original model with results from simulation where the coupling-effects are included, we would be able to study the effect the coupling-terms has on the friction of rough surfaces. We would also be able to evaluate the validity of the assumption that was made in the first place; that the coupling terms could be ignored.

However, if the coupled terms are included, the friction process can not be divided into 'vertical squeeze' and 'horizontal pull'. Both the vertical and the horizontal forces must be evaluated at the same time. We suggest the following solution:

Let us introduce two new vectors $\mathbf{u}$ and $\mathbf{f}$, where

$$\begin{aligned} \mathbf{u} &= [\mathbf{u}_z\ \mathbf{u}_x] = \begin{bmatrix} u_{z1} & u_{z2} & \cdots & u_{zN} & u_{x1} & u_{x2} & \cdots & u_{xN} \end{bmatrix} \\ \mathbf{f} &= [\mathbf{f}_z\ \mathbf{f}_x] = \begin{bmatrix} f_{z1} & f_{z2} & \cdots & f_{zN} & f_{x1} & f_{x2} & \cdots & f_{xN} \end{bmatrix} \end{aligned}$$

Equation (3.5) can then be re-formulated as:

$$\mathbf{u} \;=\; \overline{\mathbf{G}} \cdot \mathbf{f} \tag{6.1}$$

where

$$\overline{\mathbf{G}} = \begin{bmatrix} \overline{\mathbf{G}}_{zz} & \overline{\mathbf{G}}_{zx} \\ \overline{\mathbf{G}}_{xz} & \overline{\mathbf{G}}_{xx} \end{bmatrix} = \begin{bmatrix} G_{zz,11} & \cdots & G_{zz,1N} & G_{zx,11} & \cdots & G_{zx,1N} \\ \vdots & \ddots & \vdots & \vdots & \ddots & \vdots \\ G_{zz,N1} & \cdots & G_{zz,NN} & G_{zx,N1} & \cdots & G_{zx,NN} \\ G_{xz,11} & \cdots & G_{xz,1N} & G_{xx,11} & \cdots & G_{xx,1N} \\ \vdots & \ddots & \vdots & \vdots & \ddots & \vdots \\ G_{xz,N1} & \cdots & G_{xz,NN} & G_{xx,N1} & \cdots & G_{xx,NN} \end{bmatrix}$$

We introduce a matrix $\mathbf{K}$, which includes both $\mathbf{K_z}$ and $\mathbf{K_x}$; it defines both the contact area, and the area where the two surfaces are 'bound' to each other vertically:

$$\mathbf{K} = \begin{bmatrix} \mathbf{K_z} & \mathbf{0} \\ \mathbf{0} & \mathbf{K_x} \end{bmatrix} = \begin{bmatrix} K_{z,11} & 0 & 0 & 0 & 0 & 0 \\ 0 & \ddots & 0 & 0 & 0 & 0 \\ 0 & 0 & K_{z,NN} & 0 & 0 & 0 \\ 0 & 0 & 0 & K_{x,11} & 0 & 0 \\ 0 & 0 & 0 & 0 & \ddots & 0 \\ 0 & 0 & 0 & 0 & 0 & K_{x,NN} \end{bmatrix}$$

Using the boundary conditions found in section 4.5.1 and 4.6.1, we find that for a given surface profile, penetration depth D_z and horizontal pulling length D_x:

- $\mathbf{K} \cdot \mathbf{u}$ is known everywhere
- $(\mathbf{I} - \mathbf{K}) \cdot \mathbf{f}$ is zero everywhere

Using $\mathbf{K}$, we can re-formulate equation (6.1) as follows:

$$\overline{\mathbf{G}} \cdot (\mathbf{I} - \mathbf{K}) \cdot \mathbf{f} + \overline{\mathbf{G}} \cdot \mathbf{K} \cdot \mathbf{f} \;=\; (\mathbf{I} - \mathbf{K}) \cdot \mathbf{u} + \mathbf{K} \cdot \mathbf{u}$$

We introduce $\mathbf{x} \;=\; \mathbf{K} \cdot \mathbf{f} + (\mathbf{I} - \mathbf{K}) \cdot \mathbf{u}$ which contains all the unknown quantities in our system. Via the same derivation as in section 4.5.2, we arrive at the following equation:

$$(-\mathbf{I} + (\mathbf{I} + \overline{\mathbf{G}}) \cdot \mathbf{K}) \cdot \mathbf{x} \quad = \quad \mathbf{K} \cdot \mathbf{u} \tag{6.2}$$

Equation (6.2) is on the form Ax=b, and can be solved using, for example, the conjugate gradient method [32].

Now, we know how to solve the elastic equation for a given D_x, D_z, $\mathbf{K_z}$ and $\mathbf{K_x}$. However, we need to re-model the process of 'squeeze, pull and slip' .

The coupling between horizontal and vertical effects introduce some new complexities:

- both $\{f_x\}$ and $\{f_z\}$ are dependent on D_x
- the contact area $\mathbf{K_z}$ is dependent on D_x
- $f_x(D_x)$ and $f_z(D_x)$ does not go through zero. (Due to the coupling effects, there are still horizontal forces even when $D_x = 0$.)

However, the functions $f_x(D_x)$ and $f_z(D_x)$ are still linear on the intervals where both $\mathbf{K_z}$ and $\mathbf{K_x}$ is constant.

We suggest the following algorithm:

1. Generate a rough surface
2. Define a penetration depth D_z
3. Set initial contact area $\mathbf{K}_z$ equal to the slice area (see figure 4.5)
4. Initially, set $\mathbf{K}_x = \mathbf{K}_z$
5. Set $D_x = 0$
6. Solve equation 6.2, with respect to $\mathbf{x}$, to obtain all forces and displacements..
7. Iterate to find the right $(D_x = 0)$ contact area: If there are sites where $f_z < 0$
   (a) set $K_z = 0$ and $K_x = 0$ at these points
   (b) return to 6.
8. Set $D_{x0} = 0$

9. Solve equation 6.2, with respect to $\mathbf{x}$, to obtain all forces and displacements at $D_x = D_{x0}$. Calculate $F_z\left(D_{x0}\right) = \sum f_z\left(D_{x0}\right)$ and $F_x\left(D_{x0}\right) = \sum f_x\left(D_{x0}\right)$

10. Introduce a new horizontal pulling-distance D_x

11. Solve equation 6.2, with respect to $\mathbf{x}$, to obtain all forces and displacements for the new D_x. Calculate $F_z = \sum f_z$ and $F_x = \sum f_x$

12. Iterate: while there still exists lattice sites where $K_x = 1$

    (a) Find the point with the maximum fraction $\frac{f_x}{\lambda f_z}$

    (b) Find the point with the minimum f_z

    (c) Calculate the D_x needed for the first horizontal bond to break:
    $D_{x,limx} = D_x + \left(1 - max\left\{\frac{f_x}{\lambda f_z}\right\}\right) \cdot \frac{(D_x - D_{x0})}{max\left\{\frac{f_x}{\lambda f_z}\right\} - max\left\{\frac{f_x(D_{x0})}{\lambda f_z(D_{x0})}\right\}}$

    (d) Calculate the D_x at which the contact area changes:
    $D_{x,limz} = D_x + min\left\{f_z\right\} \cdot \frac{(D_x - D_{x0})}{min\{f_z(D_{x0})\} - min\{f_z\}}$

    (e) if $D_{x,limx} < D_{x,limz}$

        i. set $K_x = 0$ for the site with the maximum fraction $\frac{f_x}{\lambda f_z}$

        ii. find the total forces $F_{x,lim}$ and $F_{z,lim}$ needed for the bond to break

            A. $F_{x,lim} = F_x \cdot \frac{D_{x,limx}}{D_x}$ (the function $F_x(D_x)$ goes through zero)

            B. $F_{z,lim} = F_z + (D_{x,limx} - D_x) \cdot \frac{F_z - F_z(D_{x0})}{D_x - D_{x0}}$

        iii. set new $D_{x0} = D_{x,limx}$

        iv. return to 9.

    (f) if $D_{x,limz} < D_{x,limx}$

        i. set $K_z = 0$ and $K_x = 0$ for the site with the minimum f_z

        ii. find the total forces $F_{x,lim}$ and $F_{z,lim}$ needed for the bond to break

            A. $F_{x,lim} = F_x \cdot \frac{D_{x,limz}}{D_x}$ (this function goes through zero)

            B. $F_{z,lim} = F_z + (D_{x,limz} - D_x) \cdot \frac{F_z - F_z(D_{x0})}{D_x - D_{x0}}$

        iii. set new $D_{x0} = D_{x,limz}$

        iv. return to 9.

13. Find the friction force $F_{friction} = max\left\{F_{x,lim}\right\}$ and the maximum normal force $F_n = max\left\{F_{z,lim}\right\}$

14. Return to 1. and repeat on a defined number of samples. Average the results over the samples, to find a point in the static friction law $F_{friction} = F_{friction}\left(F_n\right)$

15. Return to 1. with another penetration depth D_z

6.2 Two rough surfaces in contact

It would be relatively easy to change our model from studying a hard rough surface in contact with an elastic half-plane, to studying a hard, rough surface in contact with an elastic, rough surface.

The boundary-conditions would still hold true:

- the deformations are known wherever there is contact
- the forces are zero wherever there is no contact

However, to find the deformations at contact points, one would have to take into consideration both the profile of the hard surface, the 'penetration depth' D_z, and the undeformed profile of the elastic surface.

This could be an useful future extension to the model. It would be interesting to study similarities and differences compared to the simplified system used in the original model. According to research done by Greenwood and Tripp in 1971 [29], a system with two rough surfaces should "increase the tolerance of non-Gaussian distributions". Expected behaviour is therefore that the exponent α in the power law $F_{friction} \propto F_n^{\alpha}$ will become closer to 1.

6.3 Fourier acceleration

As seen from section 5, more numerical work is needed in order to provide quality data for the friction of rough surfaces. Simulations should be done on much larger system sizes, and with many more samples at each data point. In order to achieve this, we recommend implementing Fourier acceleration [33, 34] which will decrease simulation times significantly.

Chapter 7

Conclusion

We have developed a model for static friction of rough elastic surfaces. A hard, rough surface is squeezed vertically into an elastic half-space, and thereafter pulled horizontally until it starts sliding.

The model is based on the theory of elasticity. As a starting point, we used a model developed by Batrouni et al [1] for vertical contact between rough elastic surfaces. We expanded this model to include horizontal forces and displacements. We also developed a model for the 'slip' process where the horizontal forces overcome the vertical ones, so that the surfaces starts sliding against each other. Coupling effects are ignored: 'vertical squeeze' and 'horizontal pull' are modelled as independent processes.

The model has been tested against known results, both against Hertz contact and against vertical contact of rough surfaces. Our results were in good agreement with the expected behaviour.

For friction of rough surfaces, our simulation results gave good fit to a power law behaviour: $F_{friction} \propto F_n^{\alpha}$. However, further numerical simulations are needed to determine the coefficient α with reasonable precision.

Bibliography

[1] A. Hansen G. G. Batrouni and J. Schmittbuhl. Elastic response of rough surfaces in partial contact. *Europhysics Letters*, 60(5):724–730, 2002.

[2] C. H. Scholz. *The Mechanics of Earthquakes and Faulting*. Cambridge University Press, 1990.

[3] C. H. Scholz. Earthquakes and friction laws. *Nature*, 391:37, 1998.

[4] W. F. Brace and J. D. Byerlee. Stick slip as a mechanism for earthquakes. *Science*, 153:990–992, 1966.

[5] G. K. A. Gilbert. A theory of the earthquakes of the great basin, with a practical application. *Americal Journal of Science*, XXVII:49–54, 1884.

[6] S. R. Brown and C. H. Scholz. Broad bandwidth study of the topography of natural rock surfaces. *Journal of Geophysical Research*, 90:12575–12582, 1985.

[7] S. R. Brown G. N. Boitnott W. L. Power, T. E. Tullis and C. H. Scholz. Roughness of natural fault surfaces. *Geophysical Research Letters*, 14:29–32, 1987.

[8] G. Lapasset E. Bouchaud and J. Planés. Fractal dimension of fractured surfaces: a universal value. *Europhysics Letters*, 13:73–79, 1990.

[9] E. L. Hinrichsen K. J. Måløy, A. Hansen and S. Roux. Experimental measurements of the roughness of brittle cracks. *Physical Review Letters*, 68:213–215.

[10] F. Schmitt J. Schmittbuhl and C. H. Scholz. Scaling invariance of crack surfaces. *Journal of Geophysical Research*, 100:5953–5973, 1995.

[11] E. Bouchaud. Scaling properties of cracks. *Jounal of Physics: Condensed Matter*, 9:4319–4344, 1997.

[12] D. Dowson. *History of Tribolgy*. Longman, 1979.

[13] G. Hänhner and N. Spencer. Rubbing and scrubbing. *Physics Today*, september 1998.

[14] S. Granick. Soft matter in a tight spot. *Physics Today*, July 1999.

[15] G. Amontons. De la resistance causée dans les machines. *Mémories de l'Academie Royale*, A:275–282, 1699.

[16] D. Tabor. Friction - the present state of our understanding. *Journal of Lubrication Technology*, 103:169–178, 1981.

[17] H. Hertz. Ueber die beruehrung fester elastiche koeper. *Journal fuer die reine und angewandte Mathematik*, 92:156–171, 1882.

[18] F. P. Bowden and T. Tabor. *The Friction and Lubrication of Solids*. Clarendon Press, 1985.

[19] J. F. Archard. Elastic deformation and the laws of friction. *Procedings of the Royal Society of London*, A243:190–205, 1957.

[20] J. A. Greenwood and J. B. P. Williamson. Contact of nominally flat surfaces. *Proceedings of the Royal Society of London*, A295:300–319, 1966.

[21] J. F. Archard D. J. Whitehouse. The properties of random surfaces of significance in their contact. *Proceedings of the Royal Society of London*, A316:97–121, 1970.

[22] D. J. Whitehouse and M. J. Phillips. Discrete properties of random surfaces. *Philosophical Transactions, The Royal Society of London*, A290:267–298, 1982.

[23] R. S. Sayles and T. R. Thomas. Surface topography as a nonstationary random process. *Nature*, 271(431-434), 1978.

[24] J. H. Dieterich and B. Kilgore. Direct observation of frictional contacts: New insigths for sliding memory effects. *Pure and Applied Geophysics*, 143:283–302, 1994.

[25] O. Ronsin and K. L. Coeyrehourcq. State, rate and temperature-dependent sliding friction of elastomers. *Proceedings of the Royal Society of London*, A, 457:1277, 2001.

[26] B. N. J. Persson. Elastoplastic contact between randomly rough surfaces. *Physical Review Letters*, 87(11), 2001.

[27] F. Bucher B. N. J. Persson and B. Chiaia. Elastic contact between randomly rough surfaces: Comparison of theory with numerical results. *Physical Review B*, 65, 2002.

[28] L. D. Landau and E. M. Lifshitz. *Theory of Elasticity*. Pergamon Press, 1986.

[29] J. A. Greenwood and J. H. Tripp. The contact of two nominally flat rough surfaces. *Procedings of the Institution of Mechanical Engineers, Tribology Group*, 185(48):625–633, 1971.

[30] J. Hulin F. Plouraboué, P. Kurowski and S. Roux. Aperture of rough cracks. *Physical Review E*, 51(3):1675–1685, 1995.

[31] J. Schmittbuhl A. Hansen and G. G. Batrouni. Distinguishing fractional and white noise in one and two dimensions. *Physical Review E*, 63, 2001.

[32] W. T. Vetterling W. H. Press, S. A. Teukolsky and B. P. Flannery. *Numerical Recipies in C: The Art of Scientific Computing*. Cambridge University Press, 1992.

[33] G. G. Batrouni and A. Hansen. Fourier acceleration of iterative processes in disrdered systems. *Journal of Statistical Physics*, 52:747, 1988.

[34] J. Schmittbuhl G. G. Batrouni, A. Hansen. Heterogeneous interfacial failure between two elastic blocks. *Physical Review E*, 65, 2002.

[35] K. L. Johnson. *Contact Mechanics*. Cambridge University Press, 1985.

Appendix A

Calculation of the discrete Green functions

The discrete Green functions are found by averaging equation (3.2) over an area a^2, which corresponds to the discretization size:

$$\widetilde{u}_z = \overline{G}_{zz}F_z + \overline{G}_{zx}F_x = \frac{1}{a^2}\int_{y-a/2}^{y+a/2}\int_{x-a/2}^{x+a/2}\frac{1+s}{2\pi E}\left\{\frac{2(1-s)}{r}F_z + \frac{(1-2s)x}{r^2}F_x\right\}dxdy$$

$$\widetilde{u}_x = \overline{G}_{xz}F_z + \overline{G}_{xx}F_x = \frac{1}{a^2}\int_{y-a/2}^{y+a/2}\int_{x-a/2}^{x+a/2}\frac{1+s}{2\pi E}\left\{-\frac{(1-2s)x}{r^2}F_z + \left(\frac{2(1-s)}{r} + \frac{2s}{r^3}\right)F_x\right\}dxdy$$

We calculate $\overline{G}_{zz}$, $\overline{G}_{zx}$, $\overline{G}_{xz}$ and $\overline{G}_{xx}$ by considering four cases:

- $\overline{G}_{zz}$: vertical displacements caused by vertical forces
- $\overline{G}_{xx}$: horizontal displacements caused by horizontal forces
- $\overline{G}_{zx}$: vertical displacements caused by horizontal forces
- $\overline{G}_{xz}$: horizontal displacements caused by vertical forces

A.1 $\overline{G}_{zz}$: vertical displacements caused by vertical forces

$$\begin{aligned}\widetilde{u}_z &= \int_{y-a/2}^{y+a/2}\int_{x-a/2}^{x+a/2}\frac{1+\sigma}{2\pi E}\cdot\frac{2(1-\sigma)}{r}F_z dxdy \\ &= \frac{1-\sigma^2}{\pi E}F_z\cdot\int_{y-a/2}^{y+a/2}\int_{x-a/2}^{x+a/2}\frac{1}{\sqrt{x^2+y^2}}dxdy\end{aligned}$$

$$= \frac{1-\sigma^2}{\pi E} F_z \cdot \int_{y-a/2}^{y+a/2} ln\left(\frac{x+a/2+\sqrt{(x+a/2)^2+y^2}}{x-a/2+\sqrt{(x-a/2)^2+y^2}}\right) dy$$

$$\Downarrow$$

$$\begin{aligned}\widetilde{u}_z = \frac{1-\sigma^2}{\pi E} F_z \cdot \Bigg\{ & (x+a/2) \cdot ln\left(\frac{y+a/2+\sqrt{(y+a/2)^2+(x+a/2)^2}}{y-a/2+\sqrt{(y-a/2)^2+(x+a/2)^2}}\right) \\ & +(y+a/2) \cdot ln\left(\frac{x+a/2+\sqrt{(y+a/2)^2+(x+a/2)^2}}{x-a/2+\sqrt{(y+a/2)^2+(x-a/2)^2}}\right) \\ & +(x-a/2) \cdot ln\left(\frac{y-a/2+\sqrt{(y-a/2)^2+(x-a/2)^2}}{y+a/2+\sqrt{(y+a/2)^2+(x-a/2)^2}}\right) \\ & +(y-a/2) \cdot ln\left(\frac{x-a/2+\sqrt{(y-a/2)^2+(x-a/2)^2}}{x+a/2+\sqrt{(y-a/2)^2+(x+a/2)^2}}\right) \Bigg\}\end{aligned}$$

where $\overline{G}_{zz} = \frac{\widetilde{u}_z}{F_z}$.
This result is also found in 'Contact Mechanics' by K. L. Johnson [35].

A.2 $\overline{G}_{xx}$: horizontal displacements caused by horizontal forces

$$\begin{aligned}\widetilde{u}_x &= \int_{y-a/2}^{y+a/2} \int_{x-a/2}^{x+a/2} \frac{1+\sigma}{2\pi E} \cdot \left(\frac{2(1-\sigma)}{r} + \frac{2\sigma x^2}{r^3}\right) F_x dx dy \\ &= \frac{(1-\sigma^2)}{\pi E} F_x \cdot \int_{y-a/2}^{y+a/2} \int_{x-a/2}^{x+a/2} \frac{1}{\sqrt{x^2+y^2}} dx dy \\ &\quad + \frac{\sigma(1+\sigma)}{\pi E} F_x \cdot \int_{y-a/2}^{y+a/2} \int_{x-a/2}^{x+a/2} \frac{x^2}{(x^2+y^2)^{3/2}} dx dy \\ &= \frac{(1-\sigma^2)}{\pi E} F_x \cdot \int_{y-a/2}^{y+a/2} \int_{x-a/2}^{x+a/2} \frac{1}{\sqrt{x^2+y^2}} dx dy \\ &\quad + \frac{\sigma(1+\sigma)}{\pi E} F_x \cdot \int_{y-a/2}^{y+a/2} \left(\frac{x+a/2}{\sqrt{(x+a/2)^2+y^2}} - \frac{x-a/2}{\sqrt{(x-a/2)^2+y^2}} + \int_{x-a/2}^{x+a/2} \frac{1}{\sqrt{x^2+y^2}} dx\right) dy\end{aligned}$$

$$= \frac{(1+\sigma)}{\pi E} F_x (1-\sigma+\sigma) \cdot \int_{y-a/2}^{y+a/2} ln\left(\frac{x+a/2+\sqrt{(x+a/2)^2+y^2}}{x-a/2+\sqrt{(x-a/2)^2+y^2}}\right) dy$$
$$+\frac{\sigma(1+\sigma)}{\pi E} F_x \cdot \int_{y-a/2}^{y+a/2} \left(\frac{x+a/2}{\sqrt{(x+a/2)^2+y^2}} + \frac{x-a/2}{\sqrt{(x-a/2)^2+y^2}}\right) dy$$

$$\Downarrow$$

$$\widetilde{u}_x = \frac{1+\sigma}{\pi E} F_x \cdot \left\{ (y+a/2) \cdot ln\left(\frac{x+a/2+\sqrt{(y+a/2)^2+(x+a/2)^2}}{x-a/2+\sqrt{(y+a/2)^2+(x-a/2)^2}}\right)\right.$$
$$+(y-a/2) \cdot ln\left(\frac{x-a/2+\sqrt{(y-a/2)^2+(x-a/2)^2}}{x+a/2+\sqrt{(y-a/2)^2+(x+a/2)^2}}\right)$$
$$+(1-\sigma)(x+a/2) \cdot ln\left(\frac{y+a/2+\sqrt{(y+a/2)^2+(x+a/2)^2}}{y-a/2+\sqrt{(y-a/2)^2+(x+a/2)^2}}\right)$$
$$\left. + (1-\sigma)(x-a/2) \cdot ln\left(\frac{y-a/2+\sqrt{(y-a/2)^2+(x-a/2)^2}}{y+a/2+\sqrt{(y+a/2)^2+(x-a/2)^2}}\right) \right\}$$

where $\overline{G}_{xx} = \frac{\widetilde{u}_x}{F_x}$.

A.3 $\overline{G}_{zx}$: vertical displacements caused by horizontal forces

$$\widetilde{u}_z = \int_{y-a/2}^{y+a/2} \int_{x-a/2}^{x+a/2} \frac{1+\sigma}{2\pi E} \cdot \frac{(1-2\sigma)x}{r^2} F_x dx dy$$
$$= \frac{(1+\sigma)(1-2\sigma)}{2\pi E} F_x \cdot \int_{y-a/2}^{y+a/2} \int_{x-a/2}^{x+a/2} \frac{x}{x^2+y^2} dx dy$$
$$= \frac{(1+\sigma)(1-2\sigma)}{2\pi E} F_x \cdot \int_{y-a/2}^{y+a/2} \frac{1}{2} ln\left(\frac{(x+a/2)^2+y^2}{(x-a/2)^2+y^2}\right) dy$$

$$\Downarrow$$

$$\begin{aligned}\widetilde{u}_z \;=\; & \tfrac{(1+\sigma)(1-2\sigma)}{2\pi E}F_x\cdot\;\left\{\frac{1}{2}(y+a/2)ln\left(\frac{(x+a/2)^2+(y+a/2)^2}{(x-a/2)^2+(y+a/2)^2}\right)\right.\\ & +\frac{1}{2}(y-a/2)ln\left(\frac{(x-a/2)^2+(y-a/2)^2}{(x+a/2)^2+(y-a/2)^2}\right)\\ & +(x+a/2)\left(arctan\left(\frac{y+a/2}{x+a/2}\right)-arctan\left(\frac{y-a/2}{x+a/2}\right)\right)\\ & \left.+(x-a/2)\left(arctan\left(\frac{y-a/2}{x-a/2}\right)-arctan\left(\frac{y+a/2}{x-a/2}\right)\right)\right\}\end{aligned}$$

where $\overline{G}_{zx}=\frac{\widetilde{u}_z}{F_x}$.

A.4 $\overline{G}_{xz}$: horizontal displacements caused by vertical forces

$$\begin{aligned}\widetilde{u}_x &= \int_{y-a/2}^{y+a/2}\int_{x-a/2}^{x+a/2}\frac{1+\sigma}{2\pi E}\cdot-\frac{(1-2\sigma)x}{r^2}F_z dxdy\\ &= -\frac{(1+\sigma)(1-2\sigma)}{2\pi E}F_z\cdot\int_{y-a/2}^{y+a/2}\int_{x-a/2}^{x+a/2}\frac{x}{x^2+y^2}dxdy\\ &= -\frac{(1+\sigma)(1-2\sigma)}{2\pi E}F_z\cdot\int_{y-a/2}^{y+a/2}\frac{1}{2}ln\left(\frac{(x+a/2)^2+y^2}{(x-a/2)^2+y^2}\right)dy\end{aligned}$$

$$\Downarrow$$

$$\begin{aligned}\widetilde{u}_x \;=\; & -\tfrac{(1+\sigma)(1-2\sigma)}{2\pi E}F_z\cdot\;\left\{\frac{1}{2}(y+a/2)ln\left(\frac{(x+a/2)^2+(y+a/2)^2}{(x-a/2)^2+(y+a/2)^2}\right)\right.\\ & +\frac{1}{2}(y-a/2)ln\left(\frac{(x-a/2)^2+(y-a/2)^2}{(x+a/2)^2+(y-a/2)^2}\right)\\ & +(x+a/2)\left(arctan\left(\frac{y+a/2}{x+a/2}\right)-arctan\left(\frac{y-a/2}{x+a/2}\right)\right)\\ & \left.+(x-a/2)\left(arctan\left(\frac{y-a/2}{x-a/2}\right)-arctan\left(\frac{y+a/2}{x-a/2}\right)\right)\right\}\end{aligned}$$

where $\overline{G}_{xz}=\frac{\widetilde{u}_x}{F_z}$.